Brain Topogr (2013) 26:468–478
DOI 10.1007/s10548-012-0266-6

ORIGINAL PAPER

# Neurons Activated During Fear Memory Consolidation and Reconsolidation are Mapped to a Common and New Topography in the Lateral Amygdala

**Hadley C. Bergstrom · Craig G. McDonald · Smita Dey · Gina M. Fernandez · Luke R. Johnson**

Received: 21 April 2012 / Accepted: 31 October 2012 / Published online: 16 January 2013


**Abstract** A key question in neuroscience is how memory is selectively allocated to neural networks in the brain. This question remains a significant research challenge, in both rodent models and humans alike, because of the inherent difficulty in tracking and deciphering large, highly dimensional neuronal ensembles that support memory (i.e., the engram). In a previous study we showed that consolidation of a new fear memory is allocated to a common topography of amygdala neurons. When a consolidated memory is retrieved, it may enter a labile state, requiring reconsolidation for it to persist. What is not known is whether the original spatial allocation of a consolidated memory changes during reconsolidation. Knowledge about the spatial allocation of a memory, during consolidation and reconsolidation, provides fundamental insight into its core physical structure (i.e., the engram). Using design-based stereology, we operationally define reconsolidation by showing a nearly identical quantity of neurons in the dorsolateral amygdala (LAd) that expressed a plasticity-related protein, phosphorylated mitogen-activated protein kinase, following both memory acquisition and retrieval. Next, we confirm that Pavlovian fear conditioning recruits a stable, topographically organized population of activated neurons in the LAd. When the stored fear memory was briefly reactivated in the presence of the relevant conditioned stimulus, a similar topography of activated neurons was uncovered. In addition, we found evidence for activated neurons allocated to new regions of the LAd. These findings provide the first insight into the spatial allocation of a fear engram in the LAd, during its consolidation and reconsolidation phase.

**Keywords** Unbiased stereology · Mapping · Micro anatomy · Stable · Topography · Pavlovian

**Electronic supplementary material** The online version of this article (doi:10.1007/s10548-012-0266-6) contains supplementary material, which is available to authorized users.

H. C. Bergstrom · L. R. Johnson (✉)
Departments of Psychiatry and Neuroscience, School of Medicine, Uniformed Services University (USU), Bethesda, MD 20814, USA
e-mail: lukejohnsonphd@gmail.com

C. G. McDonald · G. M. Fernandez
Department of Psychology, George Mason University, Fairfax, VA, USA

S. Dey · L. R. Johnson
Center for Neuroscience and Regenerative Medicine (CNRM), School of Medicine, Uniformed Services University (USU), Bethesda, MD 20814, USA

L. R. Johnson
Center for the Study of Traumatic Stress (CSTS), School of Medicine, Uniformed Services University (USU), Bethesda, MD 20814, USA

## Introduction

Memory consolidation refers to the progressive stabilization of a recently acquired memory into long-term storage (i.e., the engram) (Dudai 2004). When a stored memory is reactivated it may become labile, requiring another consolidation phase for it to persist; this memory process is termed reconsolidation (Przybyslawski and Sara 1997). A central question to memory research is the stability or persistence of the original memory, especially during reconsolidation (Dudai 2004, 2012; Nader and Hardt 2009; Nader et al. 2000b). Knowledge about the dynamic nature of memory systems is important for understanding inappropriate or maladaptive memories, such as those

associated with post-traumatic stress disorder (PTSD) (Mahan and Ressler 2012; Johnson et al. 2012).

Pavlovian fear conditioning is a commonly used behavioral paradigm to study memory consolidation and reconsolidation in both animal models and humans (Johnson et al. 2012; Curzon et al. 2009; Maren 2001). In Pavlovian fear conditioning, an emotionally neutral sensory stimulus, such as an auditory tone (conditioned stimulus or CS), gains emotional valence when paired with an innate, fear-arousing stimulus such as a foot shock (unconditioned stimulus or US). After conditioning, the CS alone can trigger a diverse repertoire of physiological and behavioral defensive responses. Research conducted over several decades has identified the lateral amygdala (LA) as a critical site within the neural substrate of Pavlovian fear conditioning (Davis 1992; Maren and Fanselow 1996; LeDoux 2000; Fanselow and LeDoux 1999).

Previously, we showed that neurons activated as a result of Pavlovian fear conditioning were spatially allocated to a reliable topography within the dorsolateral amygdala (LAd) (Bergstrom et al. 2011). These were the first data to suggest that fear memory encoding within the amygdala involves a non-random spatial distribution of neurons. There is evidence to suggest that some of the same neurons activated during fear conditioning are reactivated upon memory retrieval (Reijmers et al. 2007; Nomura et al. 2011). Based on these findings, it could be hypothesized that these neurons might share topography in the LAd. Numerous studies have examined the question of whether memory consolidation and reconsolidation employ similar or distinctly different molecular events (Alberini 2005, 2011; McKenzie and Eichenbaum 2011; Nader and Hardt 2009) and recent human fMRI data provide evidence for a stable memory trace in the hippocampus (Chadwick et al. 2010, 2011; Hassabis et al. 2009; Bonnici et al. 2012) and amygdala (Bach et al. 2011). The present study asks directly, using a rodent model and neuronal mapping, how neurons activated during two distinct fear memory stages are spatially allocated and reallocated in the LA (Tronel et al. 2005). Precise measurement and quantification of memory allocation in neural networks provide fundamental insight into the physical extent, shape and structure of the engram (Johnson and Ledoux 2004; Johnson et al. 2009; Bergstrom et al. 2011).

Topographic measurement of memory allocation was conducted by mapping the coordinates of neurons expressing a well-validated learning-induced plasticity-associated protein (phosphorylated mitogen-activated protein kinase, pMAPK) following fear memory acquisition and retrieval (Schafe et al. 1999, 2000, 2008; Duvarci et al. 2005). Measuring and statistically comparing the stability of neuron topography across different brains poses several significant technical challenges. The first challenge is brain alignment. To maximize the precision of stereotaxic alignment between different brains, neurons were mapped at a narrow coronal plane using the rapidly diverging lateral ventricle as a quantifiable anatomical landmark. The second, and equally as challenging, aspect of topographic measurement is spatial analysis. In a previous study, we devised a principal component analysis (PCA)-based technique for reducing and visualizing highly complex neuronal ensembles activated during the acquisition of Pavlovian fear conditioning (Bergstrom et al. 2011). Here, we expanded upon this PCA-based methodology by applying mass multiple comparisons with a false discovery rate (FDR) correction for statistically analyzing the topography of memory-storing cells. We applied this analytic tool to statistically compare the topography of neurons activated in the LAd during the consolidation and reconsolidation of a Pavlovian conditioned fear memory. Our findings provide some of the first detailed measurements of the topography of a fear engram and its reconsolidation in the LAd.

## Materials and Methods

### Subjects

All procedures were conducted in accordance with the National Institute of Health *Guide for the Care and Use of Experimental Animals* and were approved by the Uniformed Services University Institutional Animal Care and Use Committee. Male Sprague–Dawley rats (Taconic) weighing 225–250 g on arrival to the vivarium were group housed (2/cage) on a 12 h light:dark cycle (lights on 0600; lux 15) with food and water provided ad libitum. Bedding was changed 2/week. The vivarium humidity (55 %) and temperature (20.5 °C) was constantly maintained. Rats were allowed at least 7 days of acclimation to the vivarium and handled on 3 days prior to testing. All experiments were conducted during the light phase. Rats weighed 320 ± 9.6 g (266.5–445.7 g) at time of testing. Disclosure of housing and husbandry procedures was in accordance with recommendations for standard experimental reporting (Prager et al. 2011).

### Pavlovian Auditory Fear Conditioning

Rats ($N = 28$) were randomly subdivided into four experimental conditions (Fear conditioning, FC, $n = 7$; CS reactivated, CSr, $n = 7$; CS not reactivated, CS, $n = 7$; Box alone, Box, $n = 7$). All rats were habituated to both the fear conditioning (Context A) and testing (Context B) chambers in counterbalanced order for 10 min each, one day prior to conditioning. Context A and B were

distinguished by olfactory, visual, and tactile cues. On training day, following 3 min of acclimation in Context A, rats were presented with three pairings of an auditory CS (5 kHz, 75 dB, 20 s) that co-terminated with a foot shock US (0.6 mA, 500 ms). The mean inter-trial interval (ITI) duration was 120 s. Rats were removed from the chamber 60 s after the final stimulus presentation.

Twenty-four hours later, a randomized subset of rats were placed into Context B for three minutes and then were replayed the auditory CS for 30 s (CSr). Rats in the non-reactivated memory group (CSn) were placed into Context B for the same duration of time as the CSr group (270 s) but were not played the reminder auditory CS. A fourth group was handled, habituated and exposed to Context A and B, but did not undergo fear conditioning or memory reactivation trials (Box). An experimenter blind to the experimental condition of the animals scored animal freezing, a behavior measure of conditioned fear (Fanselow 1980), from digitized videos. For the auditory CS test, freezing was scored during the 3 min prior to the CS, during the CS (30 s), and 60 s after the CS. A mean freezing value was calculated from the freezing episodes during the presentation of the CS and transformed into a percentage freezing. Mean freezing was the dependent variable.

## pMAPK Immunohistochemistry

The presence of pMAPK in LA neurons served as a molecular indicator of neuroplasticity associated with Pavlovian auditory fear memory consolidation (Schafe et al. 1999, 2000, 2008) and reconsolidation (Duvarci et al. 2005) and see (Davis and Laroche 2006) for review.

### *Tissue Preparation*

Rats were anesthetized for perfusion exactly 60 min after auditory fear conditioning (Schafe et al. 2000) or memory reactivation. Rats were anesthetized with an intraperitoneal (i.p.) injection of a ketamine/xylazine (100, 10 mg/kg) cocktail and transcardially perfused through the ascending aorta with ice cold saline followed by ice cold 4 % paraformaldehyde/0.1 M phosphate buffer (PB) at pH 7.4 (250 mL). Brains were removed and stored in the fixative overnight (4 °C) then stored in phosphate buffered saline (PBS). Free-floating serial coronal brain sections containing the amygdala were cut on a vibratome at 60 μm. All sections were treated with 1 % sodium borohydride and washed (PBS) prior to processing for pMAPK immunoreactivity.

### *Immunohistochemistry*

Sections were first blocked in PBS containing 1 % bovine serum albumin (BSA)/0.02 % Triton X-100 for 1 h. Next, sections were incubated in a rabbit polyclonal antibody to phospho-p44/42 MAPK (Thr202/Tyr204, 1:250 dilution, Cell Signaling Technology, Boston, MA) in PBS-1 % BSA/0.02 % Triton X-100 for 24 h at room temperature. Following washing (PBS), slices for pMAPK immunoreactivity were subsequently incubated with biotinylated goat anti-rabbit IgG (1:200 dilution, Vector Laboratories, Burlingame, CA) in PBS-1 % BSA/0.02 % Triton X-100 for 30 min. Slices were then washed (PBS) again and incubated in avidin–biotin HRP complex (ABC Elite, Vector Laboratories, Burlingame, CA). After a final wash (PBS), activated neurons were developed in SG chromagen (Vector Laboratories, Burlingame, CA). Sections were mounted in numerical order on gelatin subbed slides, air dried, then dehydrated in a graded series of alcohol and xylene, and cover-slipped.

## Amygdala Alignment

Spatial analysis across different brains requires precise stereotaxic alignment. To quantitatively match sections for stereologic and spatial analyses across brains, the morphology of the LV was digitally reconstructed from four consecutive sections (−3.32 to −3.48 Bregma) (Neurolucida v10, MBF Biosciences, VT). The area of the LV was calculated (NeuroExplorer, MBF Biosciences, VT), and sections matched based on LV area (Supplemental Figure). Detailed methods for this procedure have been previously described (Bergstrom et al. 2011).

## Design-Based Stereology

All stereology was conducted by an experimenter blind to the experimental conditions. To facilitate the most accurate stereologic estimate, subjects were included into the analysis only if staining was complete across the entire extent of the sampled rostrocaudal axis. For this reason, only a subset ($n = 15$) of the entire group ($n = 24$) was sampled for stereological analysis. We used design-based stereology (the optical fractionator probe) to estimate the total number of pMAPK immuno-labeled ($pMAPK^+$) neurons in the LAd during fear memory consolidation ($n = 5$) and reconsolidation ($n = 4$). We included the CSn group ($n = 6$) in the stereological analysis to determine the specificity of pMAPK regulation to the memory. We restricted stereology to the dorsolateral nucleus of the amygdala (LAd) because previous work has indicated a critical mediating role for the LAd in Pavlovian fear (LeDoux 2000). To delineate the LAd for each section, contours were constructed (StereoInvestigator v10, MBF Biosciences, VT) by tracing the boundaries of the LAd using a digital image of the amygdala from a rat brain atlas (Paxinos and Watson 2007). The contours were positioned over the LAd using various amygdala-centric anatomical

landmarks including the distance/presence of the lateral ventricle, rhinal fissure, central amygdala, and external capsule. Thus, the area of the LAd for all sections was identical between subjects.

Estimated totals were carried out using the optical fractionator probe (StereoInvestigator v10, MBF Biosciences, Williston, VT). All sampling was conducted under a 100× (NA 1.40) oil immersion objective. For all light microscopy, Koehler illumination principles were applied. A 1-in-2 series of sections were sampled from the rostrocaudal axis of the right LAd (Bregma −2.04 through −3.60) (13 serial sections) (Paxinos and Watson 2007). The final mean section thickness was 22.26 μm (60 μm originally). Any incomplete stained or torn section was considered a random event, designated missing and then accounted for in the stereological estimate using the fractionator principle (StereoInvestigator software v10, MBF Biosciences, Williston, VT). A total of 14/195 sections (7 %) were designated as missing.

The counting frame was 60 × 60 μm, the counting grid size was 85 × 85 μm, and the dissector height was 14 μm with an upper and lower guard limit of 2 μm. An average of 211 neurons per brain was counted. The precision of our stereological counts was determined by the Gunderson and Schmitz-Hof coefficient of error (CE) equations. The average CE across all sections for the Gundersen value ($m = 1$) was 0.075 and 0.073 for the Schmitz-Hof (second estimate) equation. We used the estimated total from the mean measured thickness to estimate the size of the neuronal population. This estimate was useful because the number of counting sites was high and the frequency of $pMAPK^+$ cells was low (StereoInvestigator v10, MBF Biosciences, Williston, VT).

## Neuron Mapping

For all neuron mapping, the experimenter was blind to the experimental conditions. The (*XYZ*) coordinates of activated neurons within the right LAd were mapped under a 100× (NA 1.40) oil immersion objective using a computer based tracing system (Neurolucida v10, MBF Biosciences, VT). NeuroExplorer (MBF Biosciences, VT) was used to quantify markers (*XYZ* coordinates). To visualize the spatial distribution of activated neurons across the sampling area of the amygdala, mean density "heat" maps were constructed. Bin dimensions for the LAd measured 100 $\mu m^2$ (46 bins). Bin dimensions were calculated by the sampling area and the mean number of $pMAPK^+$ neurons ($n$) for all subjects, where (D) is twice the expected frequency of points in a random distribution (de Smith et al. 2009): $D = (\text{area}/n)^2$. Neurons that fell into each bin were counted and saved into a matrix (Origin v 8, OriginLab, Northampton, MA). Using this methodology ensured that the size and geometry of the memory matrix was unbiased. Each bin represented the total number of neurons contained within the 60 μm thick section. Thus, each bin represented the *XYZ* axis (100 × 100 × 60 μm). Values within each bin were assigned a color for visualization purposes (a "heat" map) (SigmaPlot v 12, Systat Software, San Jose. CA). A total of 1,714 neurons were mapped from a single section across all subjects. All mapping and spatial analyses were conducted on a single slice to maintain the accuracy of comparisons across different brains.

## Statistical Analyses

### *Mass Multiple Comparisons*

To statistically evaluate the memory matrix, mass univariate ANOVA with a FDR correction was conducted across all bins (46 total comparisons). The FDR is a well-validated correction for multiple comparison testing (Benjamini and Hochberg 1995) that has been applied across a wide range of neuroscience approaches, including neuroimaging (Genovese et al. 2002), electrophysiology (Groppe et al. 2011b) and genomics (Storey and Tibshirani 2003). The FDR correction provided a balance between increased statistical power and a sufficiently stringent level of statistical control over false positives (Benjamini and Hochberg 1995). The FDR is the rate that significant effects are actually null results. FDR adjusted $p$ values were termed "$q$ values (Storey and Tibshirani 2003)." The $q$ value provided a measure for the significance of each bin in terms of only bins considered significant. One issue with the FDR correction is that reducing the number of comparisons can diminish the power of the analysis (Groppe et al. 2011a). We conducted substantially fewer tests compared to the high number of tests typically conducted in ERP (Groppe et al. 2011a) and genomic studies (Storey and Tibshirani 2003). Therefore, we selected the $q$ value threshold to improve the number of correct rejections while still maintaining sufficient control over false discoveries. We set the FDR cutoff at $q \leq .1$. The $q$ value cutoff was the probability that bins deemed statistically significant were actually not significant (false positive). Therefore, setting the FDR $q$ value cutoff to .1 ensured that no more than 10 % of the significant bins were false positives. Bins with $q$ values $\leq .1$ were termed "micro-regions of interest" (MROIs). Subsequent post hoc comparisons were conducted on statistically significant bins using a planned comparisons approach. FDR corrected $p$ values were generated using R software v. 2.13.0 (Storey and Tibshirani 2003).

### *Planned Comparisons*

All statistical comparisons among experimental conditions for stereological estimates and multiple comparisons testing were conducted using one-way ANOVA. Follow-up

**Table 1** Planned contrasts

| | | |
|---|---|---|
| Multiple comparisons testing | | |
| Contrast 1 | Experimental (FC + CSr) vs. Control (Box alone + CSn) | |
| Contrast 2 | FC vs. CSr | |
| Contrast 3 | | Box alone vs. CSn |
| Stereologic estimates | | |
| Contrast 1 | Experimental (FC + CSr) vs. Control (CSn) | |
| Contrast 2 | FC vs. CSr | |

All statistical comparisons among experimental conditions for stereological estimates and multiple comparisons testing were conducted using one-way ANOVA. Follow-up analysis was based on a priori predictions using an orthogonal planned comparisons approach (two comparisons for stereological estimates and three comparisons for multiple comparisons testing)

analysis was based on a priori predictions using an orthogonal planned comparisons approach (two comparisons for stereological estimates and three comparisons for multiple comparisons testing) (Table 1). We first hypothesized that the number of activated neurons associated with memory consolidation (FC) and reconsolidation (CSr) would be greater than when the memory was not reactivated (CSn) or in the Box condition (Contrast 1). Next, we hypothesized that the Box alone and CSn groups would activate an equivalent number of $pMAPK^+$ neurons (Contrast 2). Finally, we hypothesized that FC and CSr would engage a similar number of $pMAPK^+$ neurons (Contrast 3). Based on these hypotheses, variance associated with stereological estimates was partitioned into component parts (two experimental and one control group) using the following design: [Contrast (1) FC + CSr vs. CSn] and [Contrast (2) FC vs. CSr] (Table 1). Variance associated with multiple comparisons testing was partitioned into component parts (two experimental groups and two control groups) using the following design: [Contrast (1) FC + CSr vs. CSn + Box], [Contrast (2) FC vs. CSr] and [Contrast (3) CSn vs. Box] (Table 1). To detect outliers, we applied PCA to the data set (Bergstrom et al. 2011). Cases with component scores that fell outside ±3 were removed from further analyses.

### *Measure of Percentage Overlap for Fear Memory Maps in the LAd*

Correlation analysis provided a measure for the degree of topographic overlap between memory maps. For correlation analysis, we first calculated the ratio of the mean number of neurons contained within each bin of the consolidation and reconsolidation matrices relative to a control matrix (CSn and Box alone mean). Next, the ratio measures for consolidation and reconsolidation matrices were correlated. The ratio values provided a measure for the relationship in the number of neurons in the consolidation and reconsolidation matrices relative to controls. Correlations were calculated using Pearson's $r$. All $p$ values were deemed statistically significant when less than .05. All values embedded in the text are expressed as the mean ± standard error of the mean.

## Results

### Behavior

Analysis of freezing revealed robust (76 ± 11 %) and consistent freezing response to the reminder CS ($F[2, 17] = 48.9$; $p = 8.8 \times 10^{-8}$) (Fig. 1), indicating the stored auditory fear memory was sufficiently reactivated. Low pre-CS freezing (2 ± 0.5 %) indicated that memory reactivation was specific to the auditory CS.

### Design-Based Stereology

Results from design-based stereology revealed a nearly identical total number of activated neurons from the right LAd in the memory consolidation (FC) and reconsolidation (CSr) groups (Bregma −2.04 to −3.60; 1721 ± 137 and 1705 ± 127, respectively; $p = .77$; difference = 1 %) that was significantly greater ($p = .02$) than when the previously stored fear memory was not reactivated (CSn; 1258 ± 106) (Fig. 1). For correlation analysis of the stereologic estimate and freezing behavior, one subject (CSr group) with missing behavioral data (video loss) was dropped. The stereological estimates correlated with the behavioral freezing response ($r = .80$; $p = .001$), indicating a relationship between the size of the total population of $pMAPK^+$ neurons in the LAd and the behavioral performance of each individual (Fig. 1).

### Mass Multiple Comparisons

Prior to multiple comparisons testing, two outliers were discovered (PCA, component scores ±3) and removed from the analysis. Therefore, multiple comparison testing was conducted on $N = 26$ subjects (FC, $n = 7$; CSr, $n = 5$; CSn, $n = 7$ and Box, $n = 7$) (Fig. 2). The relative difference in the total number of activated neurons mapped at a single coronal plane between consolidation and reconsolidation groups (1.3 %) was highly consistent with the stereologic estimate (1 %). This finding confirms that the mapped section was highly representative of the overall relative difference in neuronal number between memory consolidation and reconsolidation phases. Multiple comparisons testing revealed 9/46 bins (20 %) were significantly different

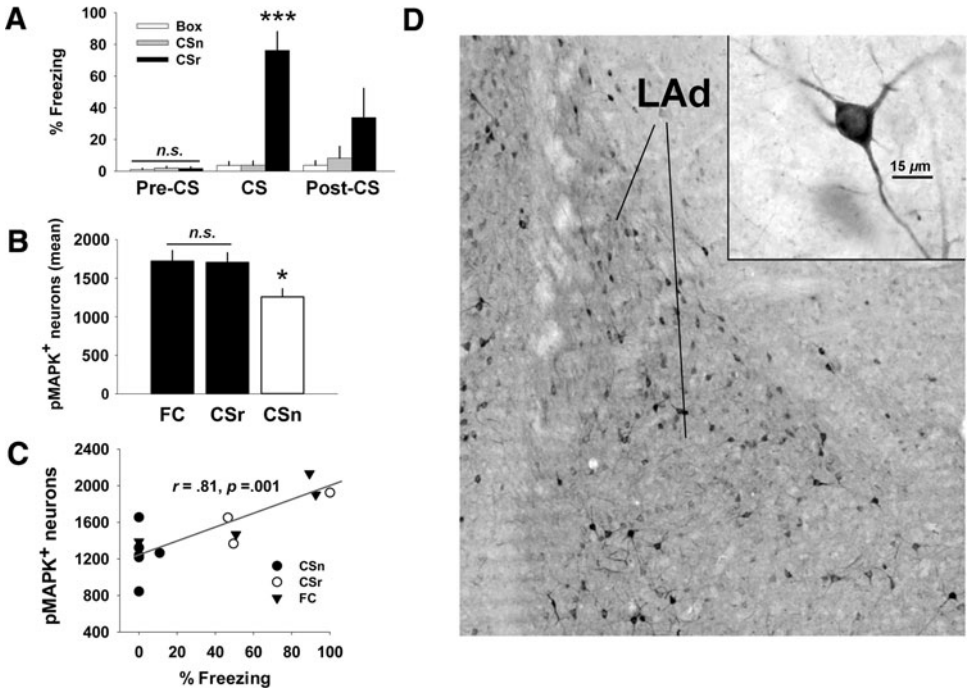


**Fig. 1** A similar quantity of activated neurons in the LAd underlies fear memory consolidation and reconsolidation. **a** Presentation of a single brief reminder CS 24 h following fear conditioning produced a robust freezing response (~70 %). **b** Stereological analysis revealed a nearly identical number of pMAPK immuno-positive neurons during fear memory reconsolidation (CSr, $n = 1705$) and consolidation (FC, $n = 1721$), that was greater than when a previously consolidated fear memory was not reactivated (CSn, $n = 1275$). **c** The number of pMAPK$^+$ neurons in the LAd for the FC, CSr and CSn groups correlated with freezing behavior ($r = .81$***). **d** Photomicrographs of pMAPK immuno-positive neurons within the LAd at (1) ×40 and ×1000 (*inset*) final magnification. Dendritic arbors are clearly visible on pMAPK immunostained neurons from the LAd. *LAd* dorsolateral amygdala. *n.s.* non-significant. *Bar graphs* reflect the mean ± SEM. *$p < .05$; ***$p < .001$

($q < .1$) between experimental conditions (Supplemental Table 1). Subsequent planned comparisons revealed an equivalent number of activated neurons in the FC and CSr groups that was significantly greater than controls in 6/9 bins (Bin 11, 14, 15, 20, 32 and 46) (Supplemental Table 2; Figs. 3, 4). Memory reconsolidation (CSr) was associated with a significantly greater number of neurons compared with consolidation (FC) and controls in 2/9 bins (Bin 25 and 26). The remaining bin (Bin 40) was specific to the FC group, with a greater number of pMAPK$^+$ neurons compared to CSr and controls. Overall, these results suggest that a majority of the neuronal activation specific to memory consolidation and reconsolidation phases was localized to a relatively small portion of the entire LAd area (20 %; 900 μm$^2$). Within this putative memory storage locus, there was a high degree of topographic overlap for the number activated neurons. Correlation analysis confirmed this conclusion, indicated a relationship ($r = .76$) for the ratio values generated from the FC and CSr memory matrices relative to controls (Fig. 3). This result provides additional confirmation for a relatively high degree of similarity in the spatial allocation of the auditory fear memory trace, during its initial encoding and after a single reactivation trial. Despite the high degree of topographic overlap, these data also indicated several loci that did not overlap, but instead were unique to either CSr (bin 25 and 26) or FC (Bin 40) phases (Figs. 3, 4).

Next, we asked what topographical features distinguished the fear memory map in the LAd. We used the $q$ value matrix (Fig. 3) as a guide for visualizing and interpreting the neuronal topography of fear memory consolidation and reconsolidation in the LAd. Several MROIs in particular (MROI 15 and 20; Figs. 3, 5), localized to the superior LAd, were identified in the $q$ value matrix. These MROIs contained significantly more activated neurons during the fear memory consolidation (MROI 15, 4.4 ± 1.0; MROI 20, 4.0 ± 0.6) and reconsolidation (MROI 15, 3.8 ± 0.2; MROI 20, 3.2 ± 1.2) phases when compared to CSn (MROI 15, 0.6 ± 0.3; MROI 20, 1.1 ± 0.3) and Box (MROI 15, 1.6 ± 0.6; MROI 20, 1.4 ± 0.7) control conditions (Fig. 4). This difference represented a threefold increase in the number of activated neurons as a result of fear memory consolidation and reconsolidation. The anatomical center of MROI 15 and 20 was located ~600 μm from the superior tip of the LAd and ~250 μm from the medial edge of the external capsule (at Bregma −3.36) (Fig. 5). The stereotaxic coordinates for these anatomical loci were highly consistent with the coordinates of an MROI that was identified in a previous

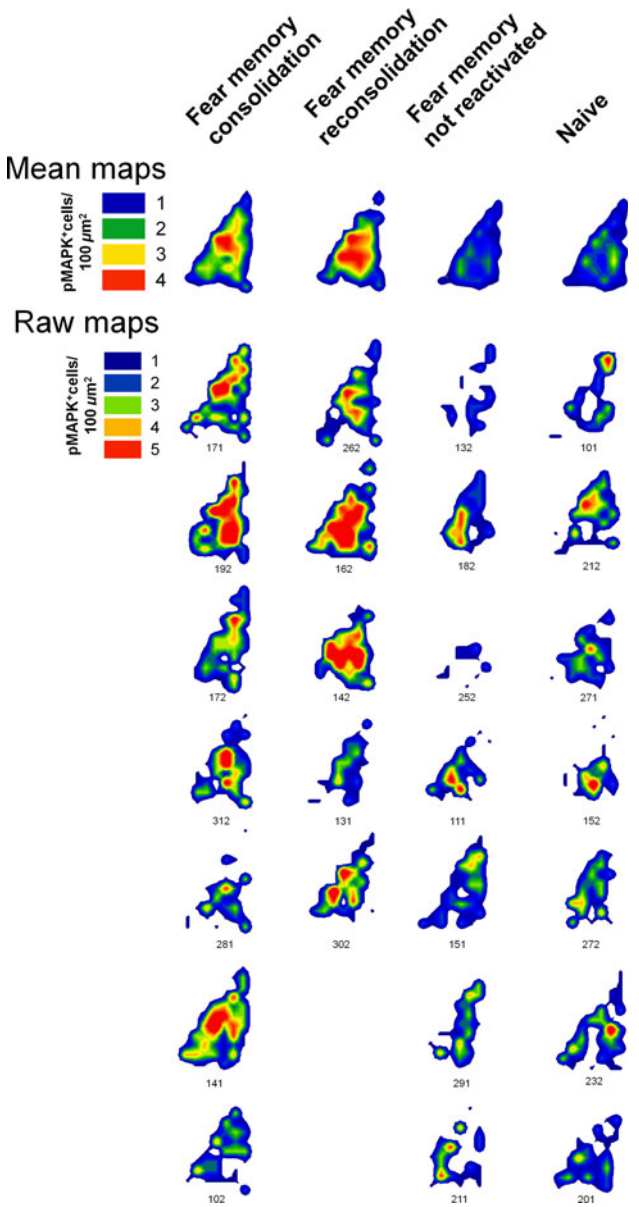


**Fig. 2** Mean and raw topographic heat maps of pMAPK$^+$ neuronal density in LAd at −3.36 Bregma. **a** Topographic heat maps of pMAPK neuronal density in the right LAd at 100 μm$^2$ spatial resolution are shown for 26 subjects. Each *map* represents the topographic distribution of pMAPK$^+$ neurons during memory consolation, reconsolidation and two control groups (non-reactivated fear memory and a Box condition). The *top row* depicts the mean values across all experimental conditions (mean maps). The *bottom rows* depict the raw values for each subject across all experimental conditions

study using an identical behavioral paradigm, but in that study there were a total of five CS–US pairings (420 μm D–V, 180 μm M–L, Bergstrom et al. 2011). There were several additional MROIs (32, and 46) in the inferior LAd that possessed significantly more neurons in the CSr and FC groups (MROI 32, 3.4 ± .65; MROI 46, 1.9 ± 0.5) compared to control conditions (MROI 32, 1.1 ± 0.3; MROI 46, 0.3 ± 0.1) (Fig. 4). The location of MROI 32 in particular (850 μm D–V, 350 μm M–L) was consistent with that identified in the previously mentioned study, although the precise coordinates differed slightly (660 μm D–V, 180 μm M–V, Bergstrom et al. 2011). It is difficult to interpret the contribution of MROI 40 to memory consolidation because the total number of activated neurons accounted for an extremely small portion (3 %) of the overall fear memory trace (Figs. 3, 4). Conversely, the number of neurons that were specific to memory reconsolidation (MROI 25 and 26) accounted for considerably more (10 %) of the overall memory trace (Figs. 3, 4). In summary, results presented here suggest the existence of a topographic fear memory map in the LAd, containing highly localized "hotspots" of plasticity at 1 h (memory consolidation) and 25 h (memory reconsolidation) post-fear conditioning, that were highly consistent (stereotyped) across individual brains.

## Discussion

Understanding how memory is spatially allocated in neural networks is a fundamental goal of neuroscience (Johnson et al. 2009). Here we found that a newly formed fear memory was allocated to a stable topography of activated neurons in the LAd. When the stored fear memory was reactivated in the presence of the relevant CS, a matching neuron population size and topography was measured. In addition, memory reactivation was associated with several locations in the LAd that were uniquely activated, suggesting new memory consolidation following retrieval. These results provide some of the first insight into the spatial allocation of a fear memory in the amygdala during its consolidation and reconsolidation phases.

We found a high degree of topographic overlap for memory consolidation and reconsolidation maps. This shared topography comprised highly localized "hotspots" containing a consistently greater number of activated neurons specific to memory consolidation and reconsolidation than surrounding areas (Figs. 3, 5). The stereotaxic coordinates of these anatomical loci were highly consistent with several other "hotspots" identified in a previous study using an identical fear conditioning paradigm, but in that study there were additional CS–US pairings (five pairings) and greater US intensity (1.0 mA) (Bergstrom et al. 2011) (Fig. 5). These findings raise the possibility that the same core memory map encodes differences in the number of CS–US pairings and the intensity of the US. Together, measures of neuronal population size and topography suggest that the neurons activated during consolidation may be some of the same neurons activated during reconsolidation. However, the present study was a between-subjects design;

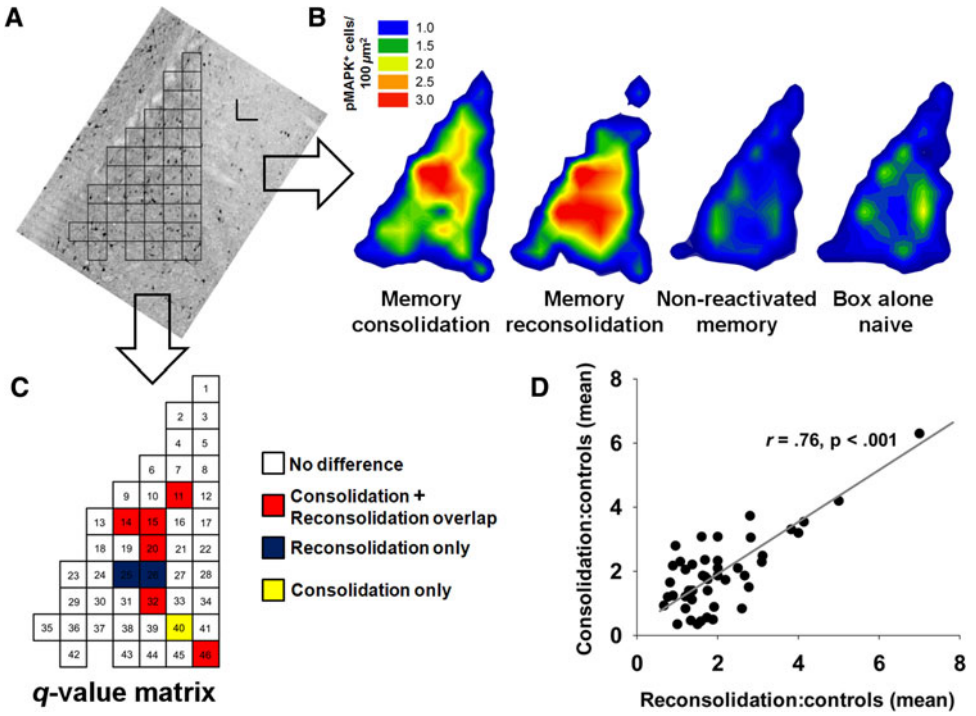


**Fig. 3** Multiple comparisons testing revealed a high degree of topographic overlap for memory consolidation and reconsolidation maps. **a** The spatial resolution (100 μm$^2$) and geometry (46 bins) of the matrix used for partitioning the LAd superimposed onto a photomicrograph of a pMAPK immunolabeled brain section. *Arrows* highlight that the same matrix was used for generating the heatmaps (*horizontal arrow*) and for multiple comparisons analysis (*vertical arrow*). **b** Topographic heat maps at 100 μm$^2$ resolution depicting the mean spatial distribution of activated neurons in the LAd from all experimental conditions at −3.36 Bregma. **c** A depiction of the *q* value matrix. *q* values ≤.1 were depicted in *color* for visualization purposes. Multiple comparisons testing (one-way ANOVA) revealed 9/46 bins (20 %) were significantly different ($q < .1$) between experimental conditions. Subsequent planned comparisons revealed that memory consolidation and reconsolidation activated an equivalent number of neurons (*red* bins) that was significantly greater than controls in 6/9 bins (Bin 11, 14, 15, 20, 32 and 46). Memory reconsolidation was associated with a significantly greater number of neurons (*blue* bins) compared with consolidation and controls in 2/9 bins (Bin 25 and 26). The remaining bin (Bin 40) was specific to consolidation, with a greater number of pMAPK$^+$ neurons (*yellow* bins) compared to reconsolidation and controls. **d** For correlation analysis, a ratio of the activated neurons in the consolidation and reconsolidation matrices relative to controls (mean) was calculated. The ratio values for the consolidation and reconsolidation groups for each bin correlated ($r = .76$; $p < .001$) (Color figure online)

therefore, it cannot directly be determined whether the same population of neurons was activated during memory consolidation and after reactivation (Johnson and Ledoux 2004; Johnson et al. 2009; Bergstrom et al. 2011). The application of cellular imaging techniques with the capability of physically tracking neurons across different memory stages will help to answer questions about whether individual neurons within a population overlap for both memory storage and retrieval. However, these techniques alone are incapable of addressing the question of precisely *which* neurons overlap for both memory phases *across individuals*. Spatial analyses, such as the mass multiple comparisons analysis used here and the PCA-based technique first developed in a previous study (Bergstrom et al. 2011), are several such complementary approaches to addressing questions about the relative stability for the location of memory-storing neurons across individual brains. Statistical comparisons of topographic measurements across individuals have the potential to shed new light onto which neurons with a population overlap for memory encoding and retrieval in the brain.

Stereologic measurement indicated a nearly identical number of neurons were activated following memory consolidation and reconsolidation that was greater than when the memory was not reactivated (Fig. 1). From these results we can infer that pMAPK activity in the reconsolidation group was due to the previously learned predictive value of the CS and not due to a non-associative aspect of the 30 s exposure to the CS. In support of this assumption, exposure to unpaired CS and US (Bergstrom et al. 2011; Schafe et al. 2000) or the CS by itself (Schafe et al. 2000) has not been found to sufficiently elevate pMAPK neuron number in the LA. Considering that pMAPK regulation in the amygdala is essential for the persistence of fear memory following reactivation (Duvarci et al. 2005), these stereology data indicate that the original fear memory underwent a process of reconsolidation when reactivated by the Pavlovian CS. Taken together, these data provide

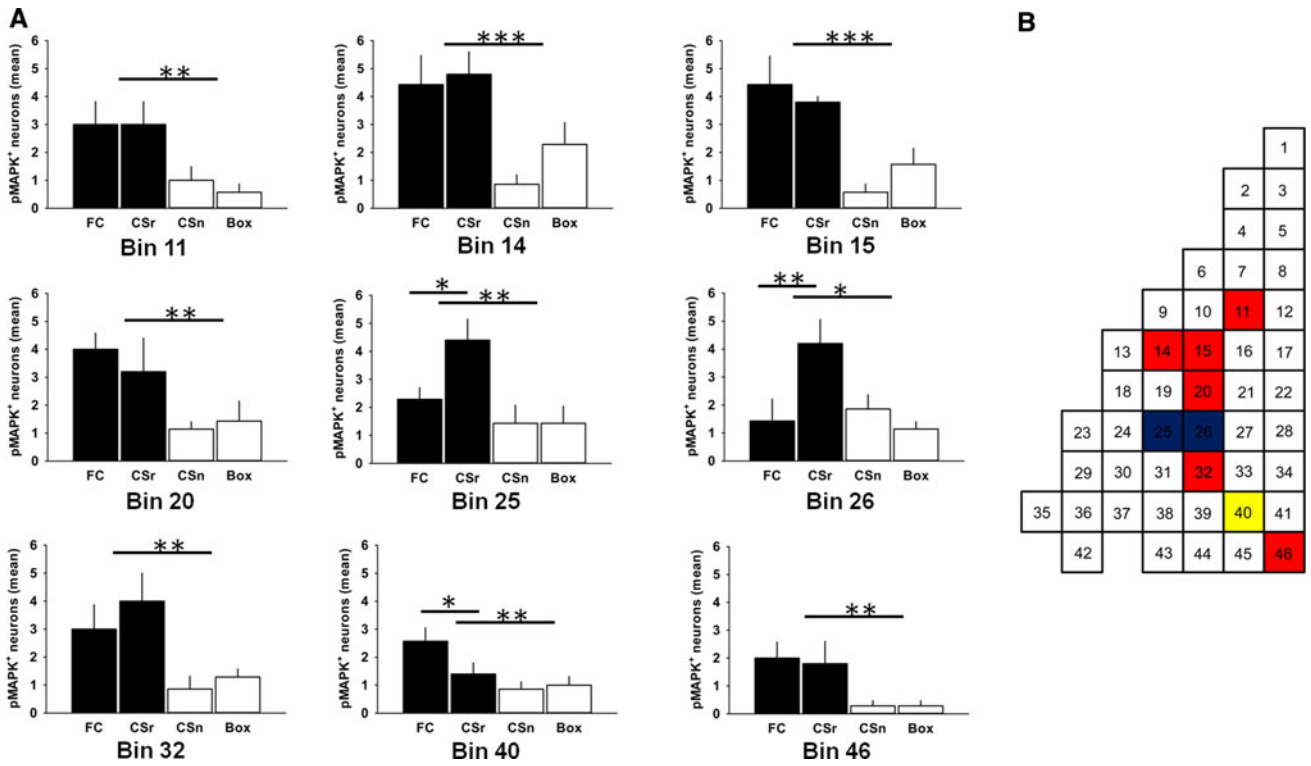


**Fig. 4** Mean number of pMAPK$^+$ neurons contained within identified micro-regions of interest in the LAd. **a** *Bar graphs* depicting the mean ± SEM number of neurons for bins with $q$ values ≤.1. **b** $q$ value matrix. *$p < .05$; **$p < .01$; ***$p < .001$

evidence that fear memory consolidation and reconsolidation engage a common population of neurons (Fig. 1). These data also indicate that non-associative or otherwise uncontrolled for processes did not activate this population.

Reconsolidation represents a mechanism that permits a stored memory to be updated in the face of new information. In addition to memory updating, new information present at the time of memory reactivation may also trigger new learning (Besnard et al. 2012; Tronel et al. 2005). Since in the present study the original memory was reactivated in a context different from that in which it was first formed, our findings do not rule out the possibility that associative learning about the new context occurred (second-order conditioning) (Tronel et al. 2005; Gewirtz and Davis 2000). A visual inspection of the spatial heat maps depicts several locations in the LAd that were uniquely activated during the reconsolidation phase (Figs. 3, 5). Spatial analyses confirmed that these loci contained a consistently greater number of activated neurons that were specific to memory reactivation (Figs. 3, 4). This finding implies that new memory consolidation processes occurred in the LAd post-retrieval. Surprisingly, new plasticity after reactivation did not translate into a larger neuronal population size, suggesting the existing memory trace partially reallocated following retrieval. Evidence for post-retrieval memory reallocation raises the intriguing possibility that the molecular signature of new memory consolidation was encoded spatially. This hypothesis requires future study aimed at whether a new second-order associative memory was indeed formed and spatial analysis of new memory consolidation for second-order associations in the LAd.

In addition, there remains a possibility that a more subtle topographic reorganization was not detectable at the spatial resolution of our analysis (Dudai 2012) (100 × 100 × 60 μm; 1.5 cells/bin across all experimental conditions). Although the existence of new learning, and therefore a degree of new mapping, during memory reconsolidation is a likely possibility, we can conclude from the present data set the existence of statistically reliable fear memory consolidation and reconsolidation maps in the LAd.

Another parameter in memory storage is the passage of time. In this experiment, 24 h elapsed between memory formation and reactivation, a temporal window that is generally considered to be outside the first consolidation phase (Nader et al. 2000a). However, there is some evidence to suggest that as time passes, memory reconsolidation processes change (Wang et al. 2009; Alberini 2011; Inda et al. 2011), including circuit reorganization at even more remote time points (Bontempi et al. 1999; Sacco and Sacchetti 2010). Whether the LAd microcircuit, as measured by quantity or topography of activated neurons, encoding a fear memory trace undergoes changes as it ages is unknown, and is a key question for future research using the methodology we have developed here.

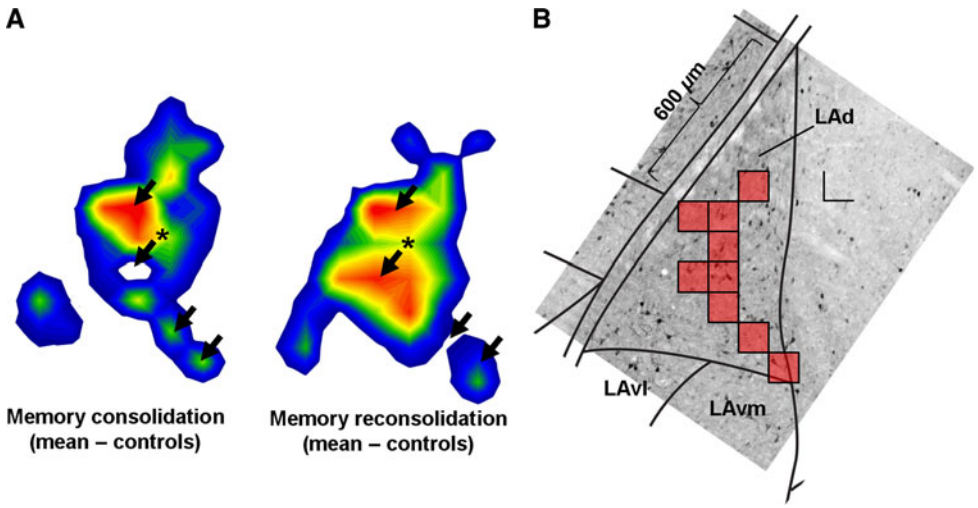


**Fig. 5** Difference heat maps for consolidation and reconsolidation in the LAd (mean–controls mean). **a** The neuronal distribution for the mean of the control groups was subtracted from the consolidation and reconsolidation maps to produce difference heat maps. The *arrowheads* depict the regions with the greatest number of activated neurons in the consolidation and reconsolidation groups. The *asterisk arrowhead* highlights the micro-region that was specific to memory reactivation. **b** Photomicrograph depicts a representative coronal section containing pMAPK immuno-labeled neurons from the LAd. Superimposed onto the photomicrograph are the anatomical boundaries of the LAd and an approximation of the stereotaxic locations of the micro regions of interest (MROI). The *scale bar* represents 100 µm for the *XY* axis

MAPK is a key memory facilitating kinase necessary for the consolidation and reconsolidation of associative fear memory in the LA (Schafe et al. 1999, 2000, 2008; Duvarci et al. 2005). MAPK phosphorylation in the LA is temporally dynamic with an initial peak at approximately 60 min post fear conditioning (Schafe et al. 2000). The temporal profile of pMAPK phosphorylation in the LA after fear memory reactivation has not yet been determined. Previous work showed that the MAPK inhibitor U0126 injected directly into the LA at 30 or 60 min prior to reactivation (Duvarci et al. 2005) or fear conditioning (Schafe et al. 2000) disrupted long-, but not short-term memory. These data indicate that the temporal profile of the MAPK molecular cascade in the LA following fear learning and memory retrieval is similar. Parametric study of MAPK phosphorylation at a higher temporal resolution is needed to resolve the question of whether fear memory consolidation and reconsolidation initiate distinct temporal signatures in the amygdala. Our data show that at one matching time point (60 min), using identical experimental parameters for fear conditioning, the quantity and topography of pMAPK immuno-labeled neurons in the LAd following the initial learning and retrieval of a recent memory (24 h old) is similar.

## Conclusion

Here, we show for the first time that a fear memory undergoing reconsolidation is redeployed into the same neuron topography within the LAd as when the memory was first formed. In addition, we uncovered a degree of new memory deployment after reactivation that was independent of the overall neuronal population size. This result suggests the core memory trace may be partially reallocated to incorporate new learning. These findings provide fundamental knowledge about the organization of the engram during consolidation and reconsolidation, and support the view that memory consolidation and reconsolidation can be both a recapitulation of the original memory and the formation of new memory in the brain (Tronel et al. 2005; McKenzie and Eichenbaum 2011). These findings pave the way for studying more complex fear memory representations in the amygdala and also modifications to memory reconsolidation. They have important implications for understanding fear memory pathologies including PTSD (Johnson et al. 2012).

**Acknowledgments** We are very grateful to Dr. Robert Ursano and the Center for the Study of Traumatic Stress (CSTS) for support. We thank Dr. Taiza Figueiredo for advice on the design of the stereology experiment.

## References

Alberini CM (2005) Mechanisms of memory stabilization: are consolidation and reconsolidation similar or distinct processes? Trends Neurosci 28(1):51–56

Alberini CM (2011) The role of reconsolidation and the dynamic process of long-term memory formation and storage. Front Behav Neurosci 5:12

Bach DR, Weiskopf N, Dolan RJ (2011) A stable sparse fear memory trace in human amygdala. J Neurosci 31(25):9383–9389
Benjamini Y, Hochberg Y (1995) Controlling the false discovery rate: a practical and powerful approach to multiple testing. J R Stat Soc B 57:289–300
Bergstrom HC, McDonald CG, Johnson LR (2011) Pavlovian fear conditioning activates a common pattern of neurons in the lateral amygdala of individual brains. PLoS One 6(1):e15698
Besnard A, Caboche J, Laroche S (2012) Reconsolidation of memory: a decade of debate. Prog Neurobiol 99(1):61–80
Bonnici HM, Kumaran D, Chadwick MJ, Weiskopf N, Hassabis D, Maguire EA (2012) Decoding representations of scenes in the medial temporal lobes. Hippocampus 22(5):1143–1153
Bontempi B, Laurent-Demir C, Destrade C, Jaffard R (1999) Time-dependent reorganization of brain circuitry underlying long-term memory storage. Nature 400(6745):671–675
Chadwick MJ, Hassabis D, Weiskopf N, Maguire EA (2010) Decoding individual episodic memory traces in the human hippocampus. Curr Biol 20(6):544–547
Chadwick MJ, Hassabis D, Maguire EA (2011) Decoding overlapping memories in the medial temporal lobes using high-resolution fMRI. Learn Mem 18(12):742–746
Curzon P, Rustay NR, Browman KE (2009) Cued and contextual fear conditioning for rodents. In: Buccafusco JJ (ed) Methods of behavior analysis in neuroscience, 2nd edn. CRC Press, Boca Raton
Davis M (1992) The role of the amygdala in fear and anxiety. Annu Rev Neurosci 15:353–375
Davis S, Laroche S (2006) Mitogen-activated protein kinase/extracellular regulated kinase signalling and memory stabilization: a review. Genes Brain Behav 5(Suppl 2):61–72
de Smith MJ, Goodchild MF, Longly PA (2009) Geospatial analysis. Matador, Leicester
Dudai Y (2004) The neurobiology of consolidations, or, how stable is the engram? Annu Rev Psychol 55:51–86
Dudai Y (2012) The restless engram: consolidations never end. Annu Rev Neurosci 35:227–247
Duvarci S, Nader K, LeDoux JE (2005) Activation of extracellular signal-regulated kinase- mitogen-activated protein kinase cascade in the amygdala is required for memory reconsolidation of auditory fear conditioning. Eur J Neurosci 21(1):283–289
Fanselow MS (1980) Conditioned and unconditional components of post-shock freezing. Pavlov J Biol Sci 15(4):177–182
Fanselow MS, LeDoux JE (1999) Why we think plasticity underlying Pavlovian fear conditioning occurs in the basolateral amygdala. Neuron 23(2):229–232
Genovese CR, Lazar NA, Nichols T (2002) Thresholding of statistical maps in functional neuroimaging using the false discovery rate. Neuroimage 15(4):870–878
Gewirtz JC, Davis M (2000) Using pavlovian higher-order conditioning paradigms to investigate the neural substrates of emotional learning and memory. Learn Mem 7(5):257–266
Groppe DM, Urbach TP, Kutas M (2011a) Mass univariate analysis of event-related brain potentials/fields I: a critical tutorial review. Psychophysiology 48(12):1711–1725
Groppe DM, Urbach TP, Kutas M (2011b) Mass univariate analysis of event-related brain potentials/fields II: simulation studies. Psychophysiology 48(12):1726–1737
Hassabis D, Chu C, Rees G, Weiskopf N, Molyneux PD, Maguire EA (2009) Decoding neuronal ensembles in the human hippocampus. Curr Biol 19(7):546–554
Inda MC, Muravieva EV, Alberini CM (2011) Memory retrieval and the passage of time: from reconsolidation and strengthening to extinction. J Neurosci 31(5):1635–1643
Johnson LR, Ledoux JE (eds) (2004) The anatomy of fear: microcircuits of the lateral amygdala. Fear and anxiety: the benefits of translational research. American Psychiatric Publishing, Washington, DC
Johnson LR, Ledoux JE, Doyere V (2009) Hebbian reverberations in emotional memory micro circuits. Front Neurosci 3(2):198–205
Johnson LR, McGuire J, Lazarus R, Palmer AA (2012) Pavlovian fear memory circuits and phenotype models of PTSD. Neuropharmacology 62(2):638–646
LeDoux JE (2000) Emotion circuits in the brain. Annu Rev Neurosci 23:155–184
Mahan AL, Ressler KJ (2012) Fear conditioning, synaptic plasticity and the amygdala: implications for posttraumatic stress disorder. Trends Neurosci 35(1):24–35
Maren S (2001) Neurobiology of Pavlovian fear conditioning. Annu Rev Neurosci 24:897–931
Maren S, Fanselow MS (1996) The amygdala and fear conditioning: has the nut been cracked? Neuron 16(2):237–240
McKenzie S, Eichenbaum H (2011) Consolidation and reconsolidation: two lives of memories? Neuron 71(2):224–233
Nader K, Hardt O (2009) A single standard for memory: the case for reconsolidation. Nat Rev Neurosci 10(3):224–234
Nader K, Schafe GE, Le Doux JE (2000a) Fear memories require protein synthesis in the amygdala for reconsolidation after retrieval. Nature 406(6797):722–726
Nader K, Schafe GE, LeDoux JE (2000b) The labile nature of consolidation theory. Nat Rev Neurosci 1(3):216–219
Nomura H, Nonaka A, Imamura N, Hashikawa K, Matsuki N (2011) Memory coding in plastic neuronal subpopulations within the amygdala. Neuroimage 60(1):153–161
Paxinos G, Watson C (2007) The rat brain in stereotaxic coordinates. Elsevier, San Diego
Prager EM, Bergstrom HC, Grunberg NE, Johnson LR (2011) The importance of reporting housing and husbandry in rat research. Front Behav Neurosci 5:38
Przybyslawski J, Sara SJ (1997) Reconsolidation of memory after its reactivation. Behav Brain Res 84(1–2):241–246
Reijmers LG, Perkins BL, Matsuo N, Mayford M (2007) Localization of a stable neural correlate of associative memory. Science 317(5842):1230–1233
Sacco T, Sacchetti B (2010) Role of secondary sensory cortices in emotional memory storage and retrieval in rats. Science 329(5992):649–656
Schafe GE, Nadel NV, Sullivan GM, Harris A, LeDoux JE (1999) Memory consolidation for contextual and auditory fear conditioning is dependent on protein synthesis, PKA, and MAP kinase. Learn Mem 6(2):97–110
Schafe GE, Atkins CM, Swank MW, Bauer EP, Sweatt JD, LeDoux JE (2000) Activation of ERK/MAP kinase in the amygdala is required for memory consolidation of pavlovian fear conditioning. J Neurosci 20(21):8177–8187
Schafe GE, Swank MW, Rodrigues SM, Debiec J, Doyere V (2008) Phosphorylation of ERK/MAP kinase is required for long-term potentiation in anatomically restricted regions of the lateral amygdala in vivo. Learn Mem 15(2):55–62
Storey JD, Tibshirani R (2003) Statistical significance for genome-wide studies. Proc Natl Acad Sci USA 100(16):9440–9445
Tronel S, Milekic MH, Alberini CM (2005) Linking new information to a reactivated memory requires consolidation and not reconsolidation mechanisms. PLoS Biol 3(9):e293
Wang SH, de Oliveira Alvares L, Nader K (2009) Cellular and systems mechanisms of memory strength as a constraint on auditory fear reconsolidation. Nat Neurosci 12(7):905–912